Electronic Supplementary Material (ESI) for Materials Advances.

Energy transfer triggered multicolor emissions in Tb^{3+}/Eu^{3+}-coacitivated $Y_2Mo_3O_{12}$ negative thermal expansion micropartices for dual-channel tunable luminescent thermometer

Peng Du*, Laihui Luo, Yafei Hou and Weiping Li

Department of Microelectronic Science and Engineering, School of Physical Science and Technology, Ningbo University, 315211 Ningbo, Zhejiang, China

Corresponding author:

E-mail: dp2007good@sina.com or dupeng@nbu.edu.cn (P. Du)

Table S1. CIE coordinate and CCT values of the YMO:$Tb^{3+}/2xEu^{3+}$ NTE microparticles.

Compounds	CIE coordinate		CCT
	x	*y*	
YMO:Tb^{3+}	0.328	0.566	5587 K
YMO:Tb^{3+}/0.02Eu^{3+}	0.429	0.485	3654 K
YMO:Tb^{3+}/0.06Eu^{3+}	0.520	0.421	2108 K
YMO:Tb^{3+}/0.10Eu^{3+}	0.578	0.380	1713 K
YMO:Tb^{3+}/0.14Eu^{3+}	0.598	0.367	1820 K
YMO:Tb^{3+}/0.18Eu^{3+}	0.614	0.355	2059 K

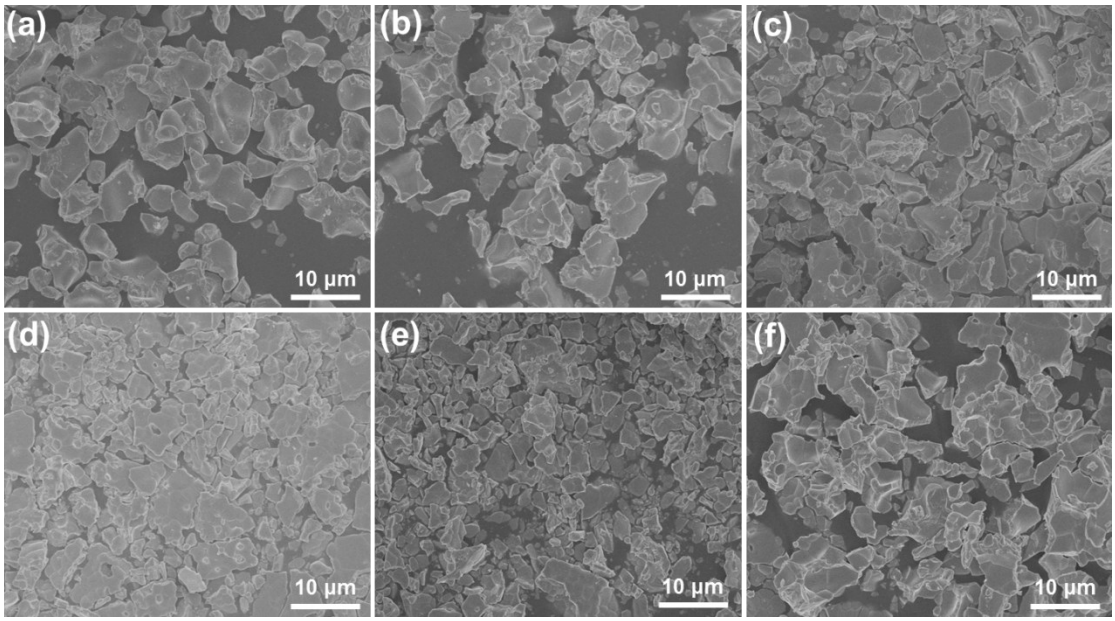

Figure S1. (a) FE-SEM image of YMO:0.06Eu^{3+} NTE microparticles. FE-SEM images of YMO:Tb^{3+}/2$x$$Eu^{3+}$ NTE microparticles with different doping concentration of (b) x = 0, (c) x = 0.01, (d) x = 0.05, (e) x = 0.07 and (f) x = 0.09.

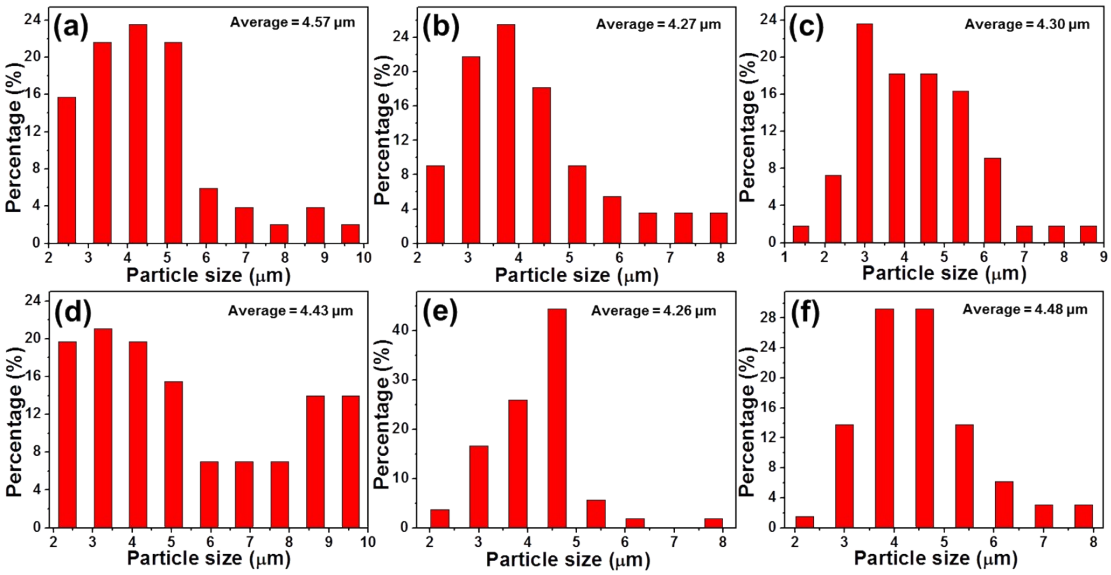

Figure S2. (a) Particle size distribution of YMO:0.06Eu^{3+} NTE microparticles. Particle size distribution of YMO:Tb^{3+}/2$x$$Eu^{3+}$ NTE microparticles with different doping concentration of (b) x = 0, (c) x = 0.01, (d) x = 0.05, (e) x = 0.07 and (f) x = 0.09.

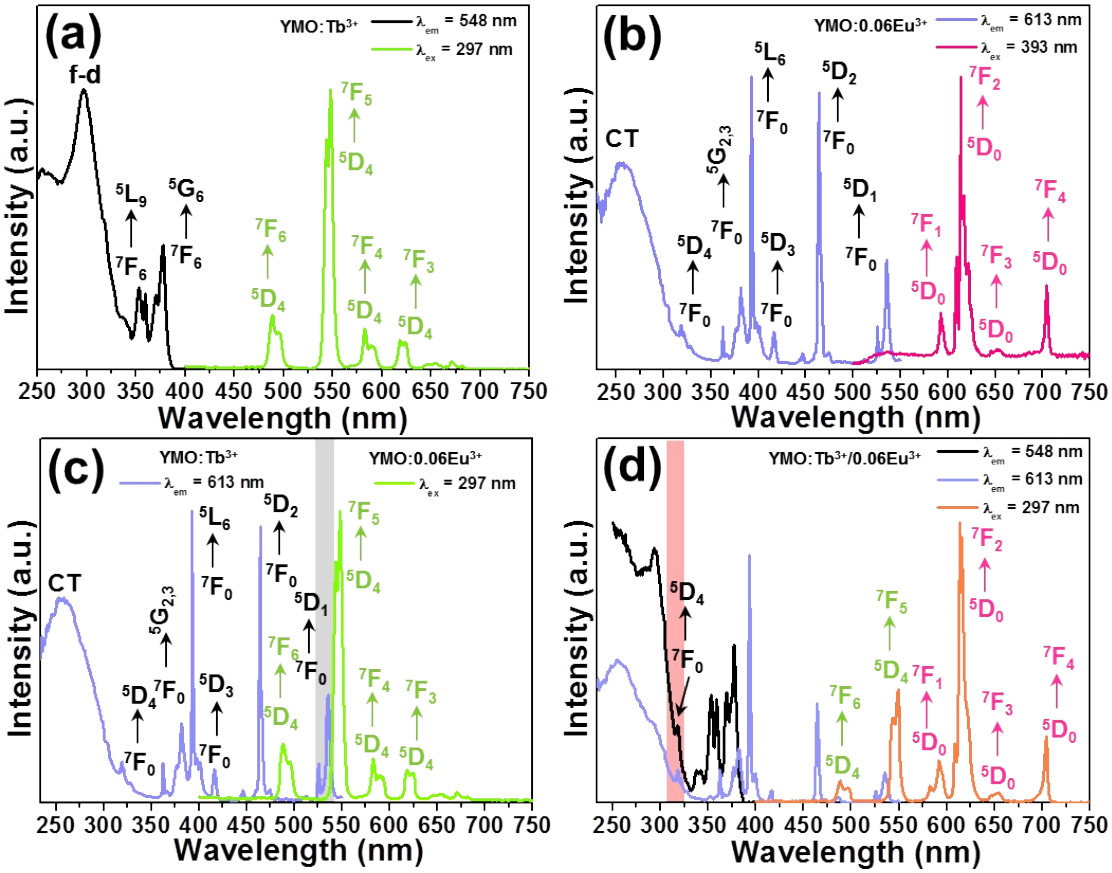

Figure S3. Excitation and emission spectra of (a) YMO:Tb^{3+} and (b) YMO:0.06Eu^{3+} NTE microparticles. (c) Excitation spectrum of YMO:0.06Eu^{3+} NTE microparticles and emission spectrum of YMO:Tb^{3+} NTE microparticles. (d) Excitation and emission spectra of YMO:Tb^{3+}/0.06Eu^{3+} NTE microparticles.

Fig. S3(a) shows the excitation and emission spectra of YMO:Tb^{3+} NTE microparticles. The excitation spectrum monitored at 548 nm is composed of an intense broad band and two sharp bands. Herein, the broad band at 297 nm is assigned to f-d transition of Tb^{3+} ions, while these two narrow peaks at 353 and 378 nm are ascribed to the transitions of $^7F_6 \rightarrow {}^5L_9$ and $^7F_6 \rightarrow {}^5G_8$, respectively.[1] Since the excitation band at 297 nm shows the strongest intensity, we use it as the excitation wavelength. Upon 297 nm excitation, only the featured emissions of Tb^{3+} ions are seen in the YMO:Tb^{3+} NTE microparticles (see Fig. S3(a)). The emission bands at 487, 548, 582 and 618 nm are assigned to the $^5D_4 \rightarrow {}^7F_6$, $^5D_4 \rightarrow {}^7F_5$, $^5D_4 \rightarrow {}^7F_4$ and $^5D_4 \rightarrow {}^7F_3$ transitions of Tb^{3+} ions, respectively.[1]

The excitation and emission spectra of the YMO:0.06Eu^{3+} NTE microparticles

are shown in Fig. S3(b). When the monitoring wavelength is 613 nm, the excitation spectrum can be divided into two parts, namely, the broad band at 256 nm is attributed to the charge transfer (CT) transition of $O^{2-} \rightarrow Eu^{3+}$, whereas these sharp peaks at 319, 363, 377, 381, 393, 416, 464 and 535 nm originating from the transitions of Eu^{3+} ions from $^7F_0$ to $^5D_4$, $^5G_2$, $^5G_3$, $^5L_6$, $^5D_3$, $^5D_2$ and $^5D_1$,[2] respectively. Excited by 393 nm, the YMO:0.06Eu^{3+} NTE microparticles only emit the featured emissions of Eu^{3+} ions and emission bands located at 593, 613, 652 and 705 nm corresponding to the $^5D_0 \rightarrow {}^7F_1$, $^5D_0 \rightarrow {}^7F_2$, $^5D_0 \rightarrow {}^7F_3$ and $^5D_0 \rightarrow {}^7F_4$ transitions.[2]

As we known, spectral overlap between the emission of Tb^{3+} ions and excitation of Eu^{3+} ions is the necessary prerequisite to the occurrence of ET from Tb^{3+} to Eu^{3+} ions in Tb^{3+}/Eu^{3+} co-activated phosphors.[3] Considering this, the excitation spectrum of YMO:0.06Eu^{3+} NTE microparticles and emission spectrum of YMO:Tb^{3+} NTE microparticles are shown in Fig. S3(c). As disclosed, the emission band of Tb^{3+} ions at 548 nm is overlapped with the excitation band of Eu^{3+} ions arising from $^7F_0 \rightarrow {}^5D_1$ transition, suggesting that the energy is able to be transferred from Tb^{3+} to Eu^{3+} ions. To further confirm the existence of ET between Tb^{3+} and Eu^{3+} ions in the Tb^{3+}/Eu^{3+}-coactivated YMO NTE compounds, we measured the excitation and emission spectra of the representative YMO:Tb^{3+}/0.06Eu^{3+} NTE microparticles, as shown in Fig. S3(d). Compared with the YMO:Tb^{3+} NTE microparticles (see Fig. S3(a)), an extra excitation band at 319 nm originating from Eu^{3+} ions is seen in the YMO:Tb^{3+}/0.06Eu^{3+} NTE microparticles aside from these bands from Tb^{3+} ions when the monitoring wavelength is 548 nm corresponding to the emission band of Tb^{3+} ions. Furthermore, upon 297 nm excitation, both the characteristic emissions of Tb^{3+} and Eu^{3+} ions are observed in the prepared samples. These results suggest that the energy can be transfer from Tb^{3+} to Eu^{3+} ions in the YMO:Tb^{3+}/2$x$$Eu^{3+}$ NTE microparticles.

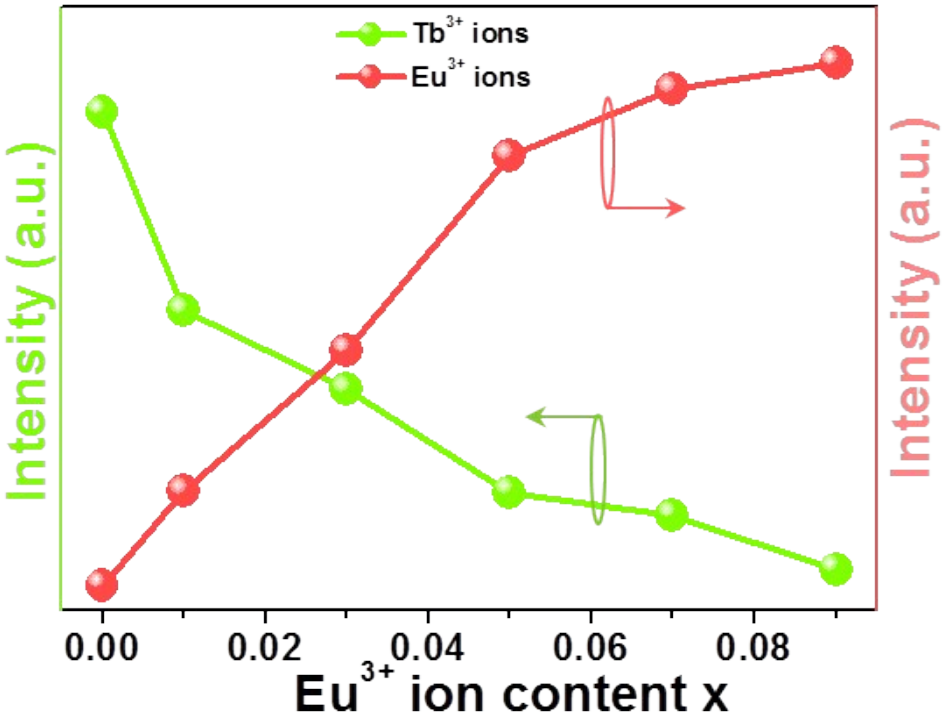

Figure S4. Emission intensities of Tb^{3+} and Eu^{3+} ions in YMO:Tb^{3+}/2*x*Eu^{3+} NTE microparticles as a function of doping concentration.

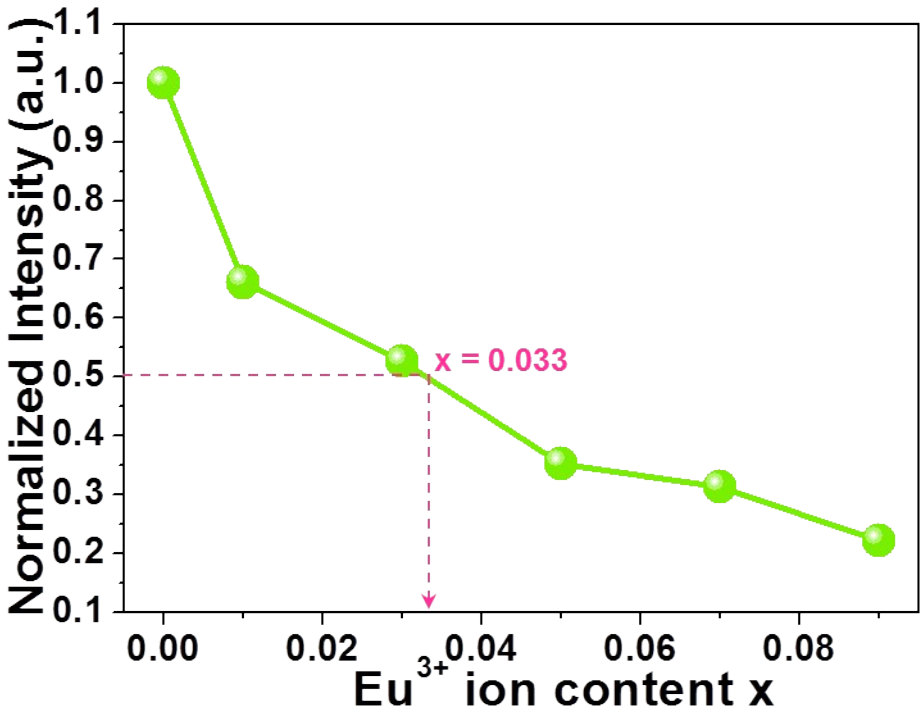

Figure S5. Normalized emission intensity of Tb^{3+} ions in YMO:Tb^{3+}/2$x$$Eu^{3+}$ NTE microparticles as a function of Eu^{3+} ion content.

As we know, the energy transfer between the sensitizer and activator is able to be realized via either exchange interaction or multipolar interaction, which can be judged by evaluating critical distance (R_c) between dopants. As previously proposed, the R_c value can be calculated by the following expression:[4]

$$R_c = 2\left[3V/4\pi x_c Z\right]^{1/3}$$

where V and N are the volume per unit cell and number of host cations in the unit cell, respectively, whereas x_c is total critical concentration of Tb^{3+} and Eu^{3+} ions, in which the content of Eu^{3+} ions corresponds to the emission intensity of Tb^{3+} ion decrease to half of its initial value without Eu^{3+} ions. From Fig. S5, one knows that the emission intensity of Tb^{3+} declines to half of its initial value when x = 0.033. In terms of YMO host, the values of V and Z are 1380.82 $Å^3$ and 4, respectively, while the total concentration of x_c is 0.063. Thus, R_c value of YMO:Tb^{3+}/2$x$$Eu^{3+}$ NTE microparticles is 32.04 Å, which is much larger than 5 Å, indicating that the involved ET mechanism between Tb^{3+} and Eu^{3+} ions is dominated by multipolar interaction.

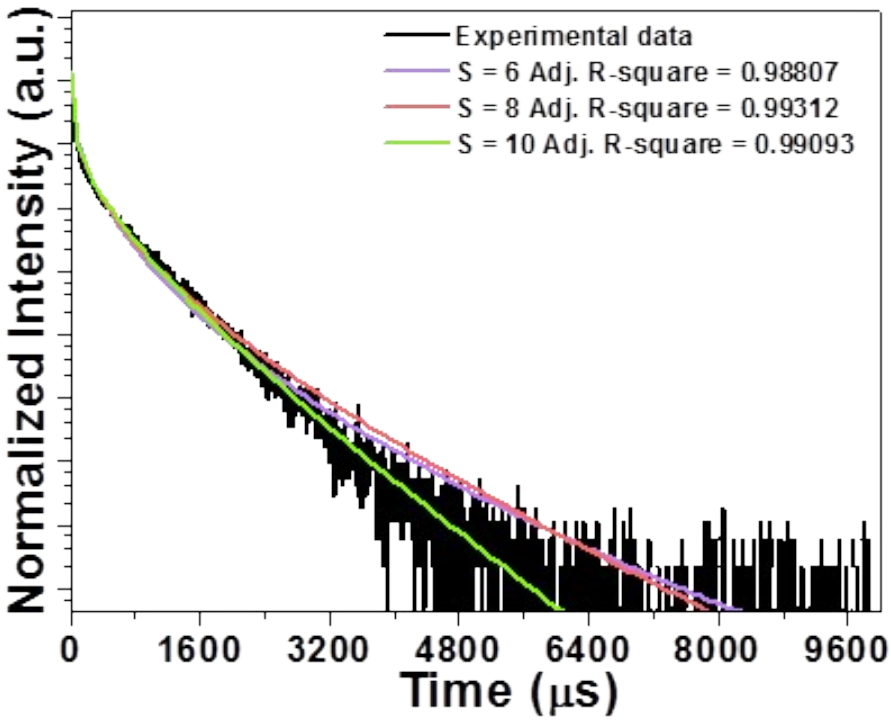

Figure S6. Fitted decay curve of YMO:Tb^{3+}/0.18Eu^{3+} NTE microparticles monitored at 378 nm by using the I-H model

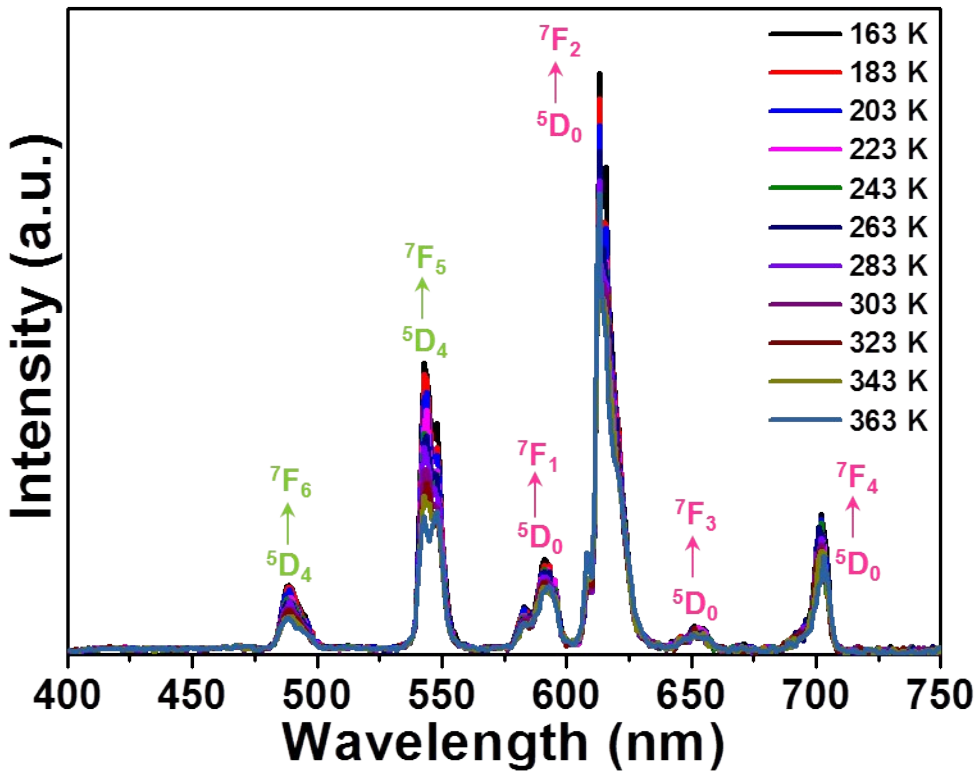

Figure S7. Emission spectra of the YMO:Tb^{3+}/0.06Eu^{3+} NTE microparticles excited by 297 nm as a function of temperature.

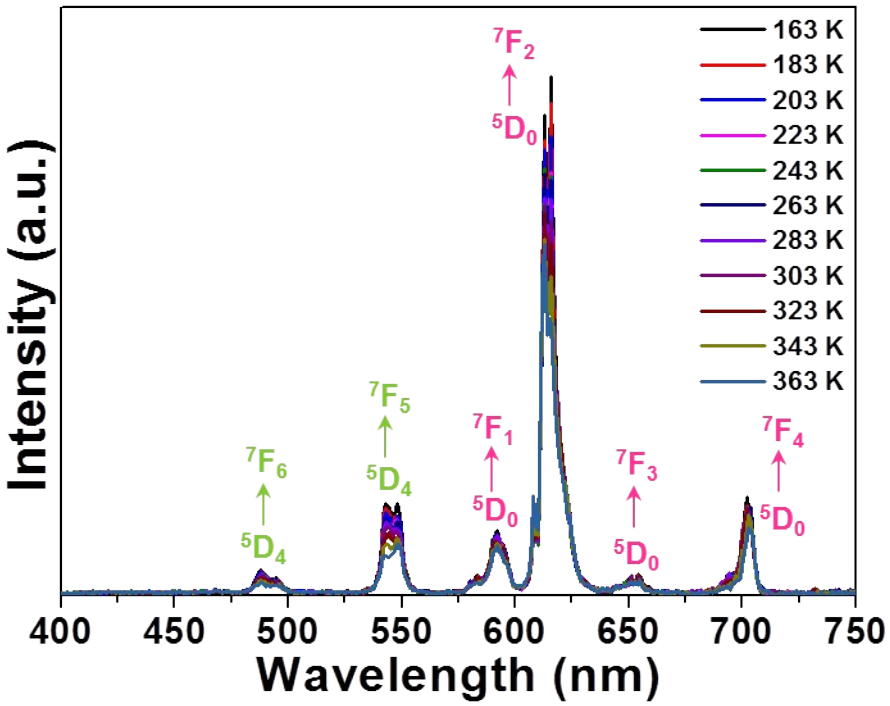

Figure S8. Emission spectra of the YMO:Tb^{3+}/0.10Eu^{3+} NTE microparticles excited by 297 nm as a function of temperature.

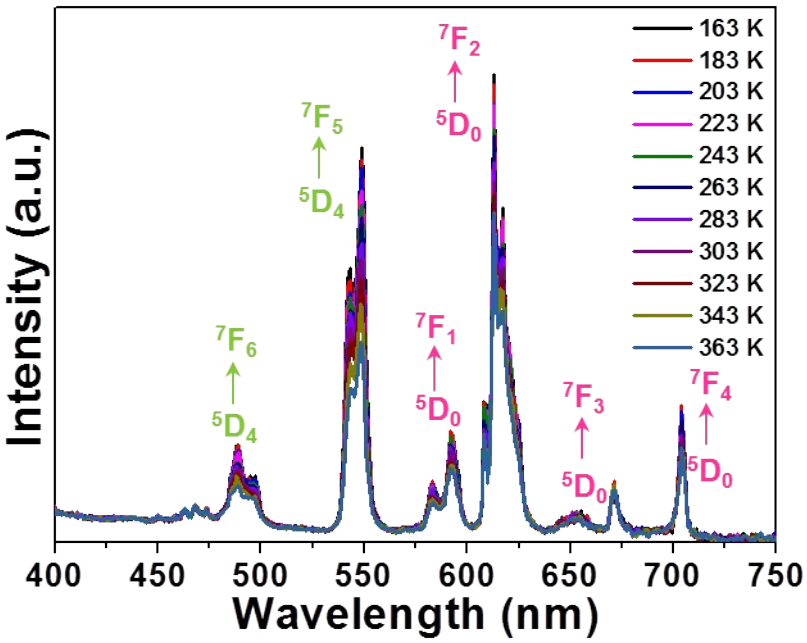

Figure S9. Emission spectra of the YMO:Tb^{3+}/0.06Eu^{3+} NTE microparticles excited by 378 nm as a function of temperature.

Reference

(1) X. Liu, X. Chen, Y. Yu, W. Xie, Y. Zhao, S. Luo, G Mei, J. Lin, *Inorg. Chem*. **2020**, 59, 12348-12361.

(2) X. Li, Y. Yu, J. Hong, Z. Feng, X. Guan, D. Chen, Z. Zheng, *J. Lumin*. **2020**, *219*, 116897.

(3) X. Huang, J. Liang, S. Rtimi, B. Devakumar, Z. Zhang, *Chem. Eng. J*. **2021**, *405*, 126950.

(4) X. Tong, J. Han, Z. Cheng, P. Wu, X. Zhang, *J. Lumin*. **2019**, *215*, 116670.